Figure S1

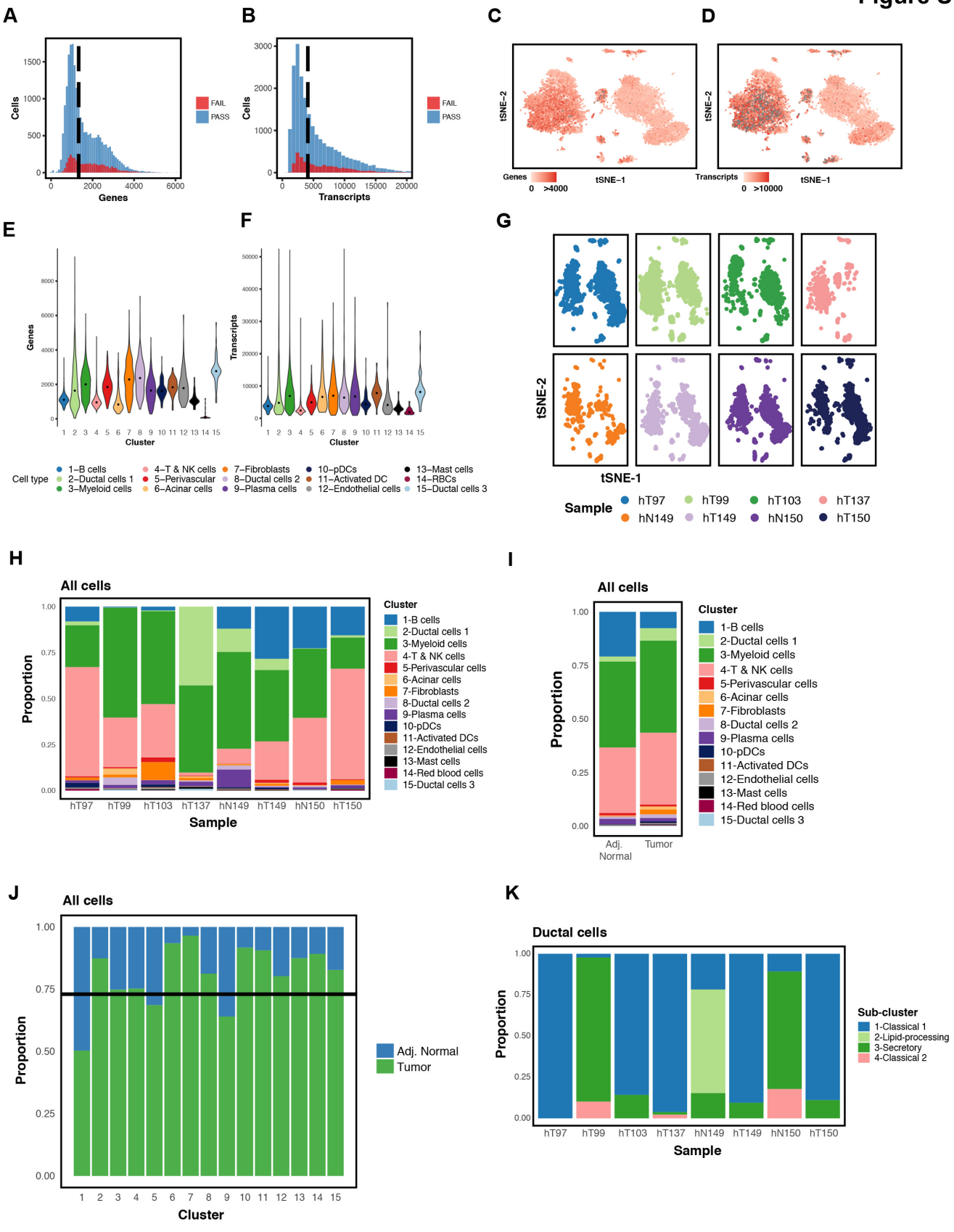
A
B
C
D
Cells
Genes
Transcripts
FAIL
PASS
tSNE-2
tSNE-1
Genes
Transcripts
0
>4000
>10000
E
F
G
Cluster
Cell type
1–B cells
2–Ductal cells 1
3–Myeloid cells
4–T & NK cells
5–Perivascular
6–Acinar cells
7–Fibroblasts
8–Ductal cells 2
9–Plasma cells
10–pDCs
11–Activated DC
12–Endothelial cells
13–Mast cells
14–RBCs
15–Ductal cells 3
Sample
hT97
hT99
hT103
hT137
hN149
hT149
hN150
hT150
H
I
All cells
Proportion
Sample
Cluster
1-B cells
2-Ductal cells 1
3-Myeloid cells
4-T & NK cells
5-Perivascular cells
6-Acinar cells
7-Fibroblasts
8-Ductal cells 2
9-Plasma cells
10-pDCs
11-Activated DCs
12-Endothelial cells
13-Mast cells
14-Red blood cells
15-Ductal cells 3
Adj. Normal
Tumor
J
K
Ductal cells
Adj. Normal
Tumor
Sub-cluster
1-Classical 1
2-Lipid-processing
3-Secretory
4-Classical 2

Supplementary Figure S1: Data quality and clustering metrics of the human PDAC single cell transcriptomes. A-B. Histograms showing the number of genes (**A**) and transcripts (**B**) that were detected per cell in the human PDAC dataset. Blue histogram shows cells that passed quality control (QC) and red histogram shows cells that failed QC. The dotted line represents the median value, which is 1,279 genes/cell and 3,938 transcripts/cell. **C-D.** Number of genes (**C**) and transcripts (**D**) detected per cell, represented as a t-SNE plot. Legend shows a color gradient corresponding to genes/transcripts number per cell. Gray color represents cells with greater than 4,000 genes or 10,000 transcripts, respectively. **E-F.** Distribution of genes (**E**) and transcripts (**F**) detected in each cluster in the human PDAC dataset. **G-H.** Patient contribution to each cluster, represented as separate t-SNE plots (**G**) and as bar plot (**H**) showing proportions of the different clusters in each sample. **I-J.** Bar plots comparing proportions of the different clusters between adjacent-normal and tumor samples, shown as clusters in each sample type (**I**) or sample types in each cluster (**J**)**.** The horizontal black line in **J** represents the input contribution of adjacent-normal or tumor tissues into the dataset. **K.** Bar plot showing proportions of the different ductal cell sub-clusters in each human sample.

Figure S2

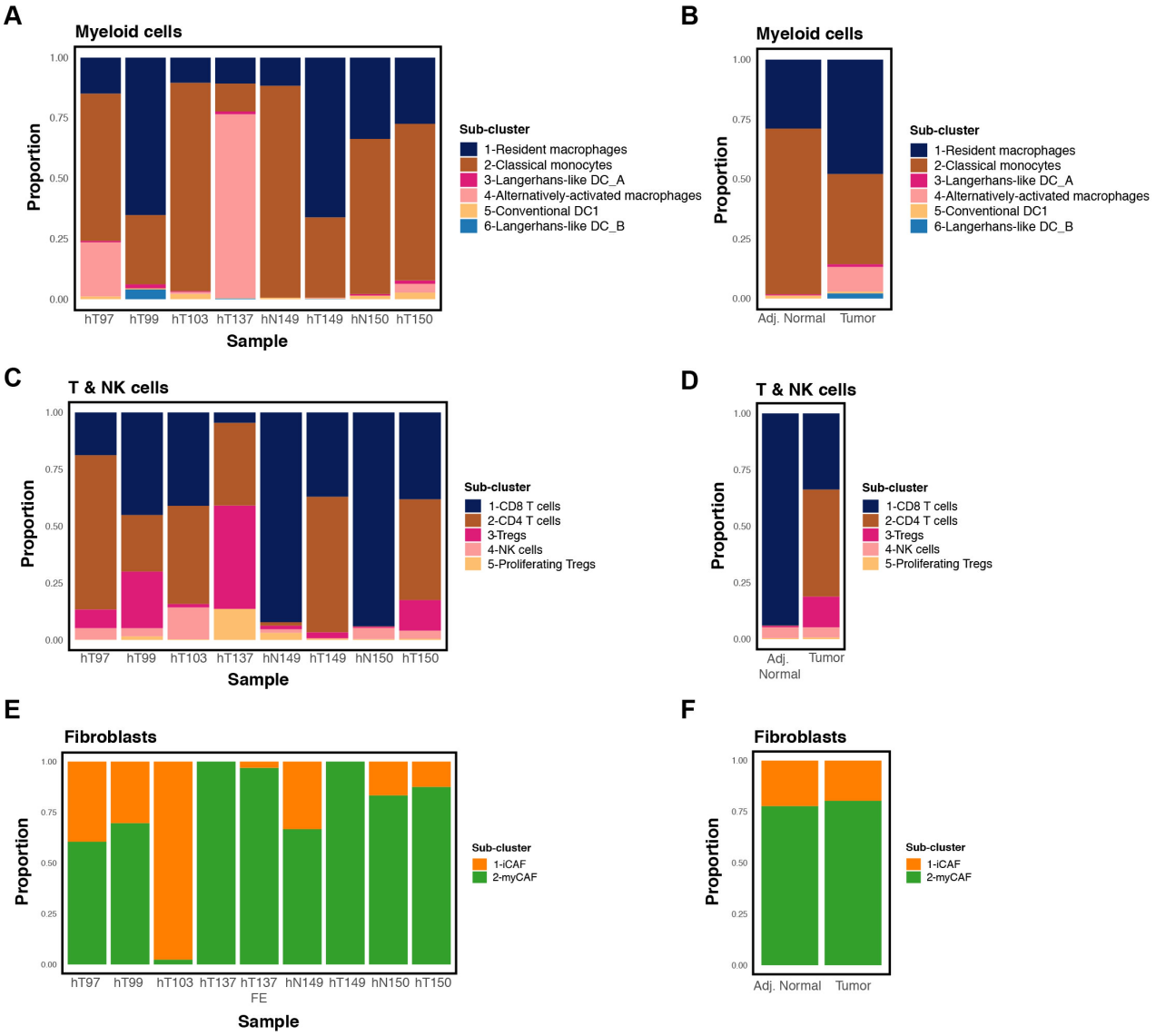

Supplementary Figure S2: Distribution of sub-clusters of cells throughout the human dataset. A. Bar plot showing proportions of the different myeloid cell sub-clusters in each human sample. **B.** Bar plot comparing proportions of the different myeloid cell sub-clusters between adjacent-normal and tumor samples. **C.** Bar plot showing proportions of the different T & NK cell sub-clusters in each human sample. **D.** Bar plot comparing proportions of the different T & NK cell sub-clusters between adjacent-normal and tumor samples. **E.** Bar plot showing proportions of the different fibroblast sub-clusters in each human sample. FE, fibroblast-enriched population. **F.** Bar plot comparing proportions of the different fibroblast sub-clusters between adjacent-normal and tumor samples.

Figure S3

A

Pathways upregulated in human myCAFs vs. iCAFs

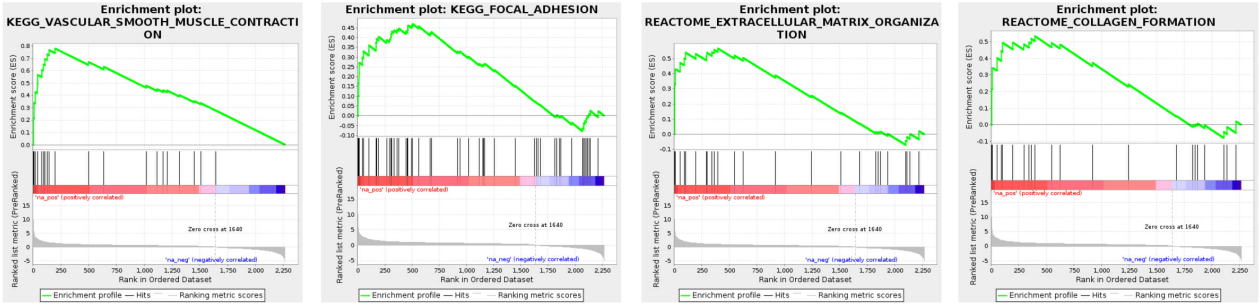

FDR q-value = 0.000
NES = 2.46

FDR q-value = 0.091
NES = 1.89

FDR q-value = 0.080
NES = 1.90

FDR q-value = 0.216
NES = 1.73

B

Pathways downregulated in human myCAFs vs. iCAFs

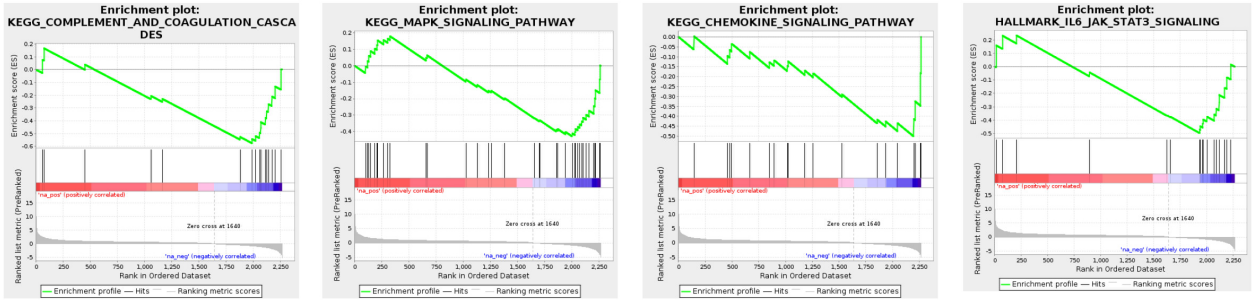

FDR q-value = 0.036
NES = -1.96

FDR q-value = 0.064
NES = -1.81

FDR q-value = 0.047
NES = -1.75

FDR q-value = 0.019
NES = -1.72

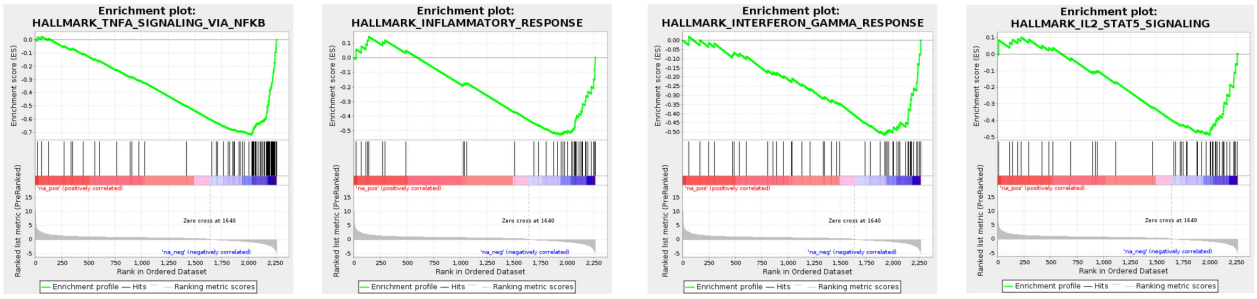

FDR q-value = 0.000
NES = -3.64

FDR q-value = 0.000
NES = -2.29

FDR q-value = 0.000
NES = -2.29

FDR q-value = 0.000
NES = -2.20

Supplementary Figure S3: Pathway analysis in human iCAFs and myCAFs. Gene set enrichment analysis (GSEA) of human myCAFs vs. human iCAFs. Shown are pathways significantly upregulated in myCAFs (**A**) or significantly downregulated in myCAFs (**B**), compared to iCAFs.

Figure S4

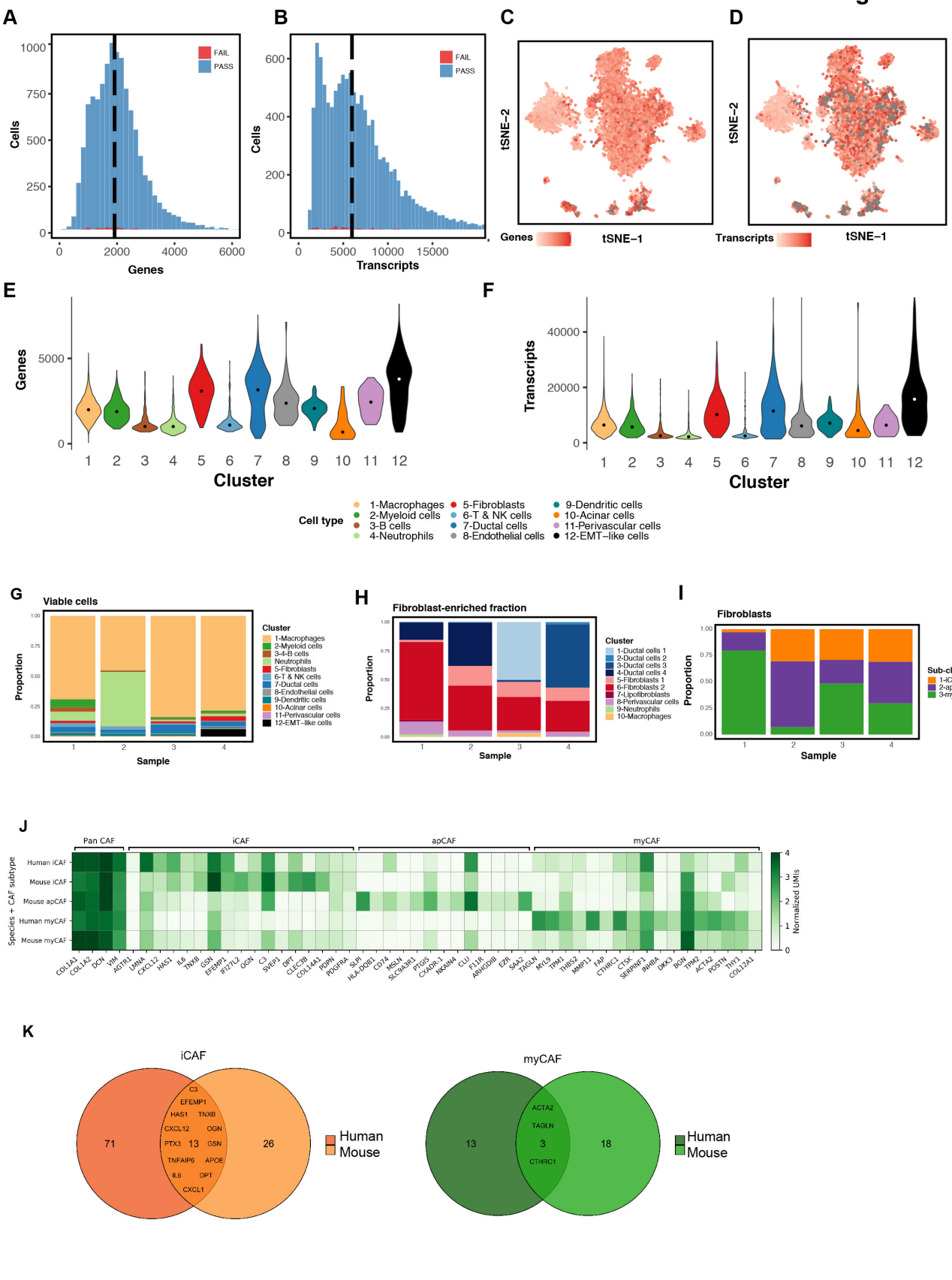
A
B
C
D
FAIL
PASS
Cells
Genes
Transcripts
tSNE-2
tSNE-1
E
F
Cluster
Cell type
1-Macrophages
2-Myeloid cells
3-B cells
4-Neutrophils
5-Fibroblasts
6-T & NK cells
7-Ductal cells
8-Endothelial cells
9-Dendritic cells
10-Acinar cells
11-Perivascular cells
12-EMT-like cells
G
Viable cells
Proportion
Sample
H
Fibroblast-enriched fraction
1-Ductal cells 1
2-Ductal cells 2
3-Ductal cells 3
4-Ductal cells 4
5-Fibroblasts 1
6-Fibroblasts 2
7-Lipofibroblasts
8-Perivascular cells
9-Neutrophils
10-Macrophages
I
Fibroblasts
Sub-cluster
1-iCAF
2-apCAF
3-myCAF
J
Pan CAF
iCAF
apCAF
myCAF
Species + CAF subtype
Human iCAF
Mouse iCAF
Mouse apCAF
Human myCAF
Mouse myCAF
Normalized UMIs
COL1A1 COL1A2 DCN VIM AGTR1 LMNA CXCL12 HAS1 IL6 TNXB GSN EFEMP1 IFI27L2 OGN C3 SVEP1 DPT CLEC3B COL14A1 PDPN PDGFRA SLPI HLA-DQB1 CD74 MGLN SLC9A3R1 PTGIS CXADR-1 NKAIN4 CLU F11R ARHGDIB EZR SAA2 TAGLN MYL9 TPM1 THBS2 MMP11 FAP CTHRC1 CTSK SERPINE1 INHBA DKK3 BGN TPM2 ACTA2 POSTN TNY1 COL12A1
K
iCAF
71
C3
EFEMP1
HAS1
TNXB
CXCL12
OGN
PTX3
13
GSN
TNFAIP6
APOE
IL6
DPT
CXCL1
26
Human
Mouse
myCAF
13
ACTA2
TAGLN
3
CTHRC1
18
Human
Mouse

Supplementary Figure S4: Data quality and clustering metrics of the KPC mouse PDAC single cell transcriptomes. A-B. Histograms showing the number of genes (**A**) and transcripts (**B**) that were detected per cell in the mouse PDAC dataset. Blue histogram shows cells that passed QC and red histogram shows cells that failed QC. The dotted line represents the median value, which is 1,916 genes/cell and 5,989 transcripts/cell**. C-D.** Number of genes (**C**) and transcripts (**D**) detected per cell, represented as a t-SNE plot. Legend shows a color gradient corresponding to gene/transcript number per cell. Gray color represents cells with greater than 4,000 genes or 10,000 transcripts, respectively. **E-F.** Distribution of genes (**E**) and transcripts (**F**) detected in each cluster in the mouse PDAC dataset. **G.** Bar plot showing proportions of the different clusters in each KPC mouse sample in the 'viable cell fraction' analysis. **H.** Bar plot showing proportions of the different clusters in each KPC mouse sample in the 'fibroblast-enriched fraction' analysis. **I.** Bar plot showing proportions of the different fibroblast sub-clusters in each KPC mouse sample. **J.** Heatmap showing orthologous genes expressed in the CAF subtypes across different species. Raw counts matrices from human and mouse CAFs were concatenated along a set of common orthologues (provided by Ensemble, described here: http://www.ensembl.info/2009/01/21/how-to-get-all-the-orthologous-genes-between-two-species/) and were normalized and log transformed jointly. **K.** Venn diagram of the common markers of iCAFs and myCAFs between human and mouse datasets, informed by marker genes for each species subtypes (from Supplementary Tables S13 and S22).

Figure S5

A

Pathways upregulated in mouse iCAFs vs. myCAFs & apCAFs

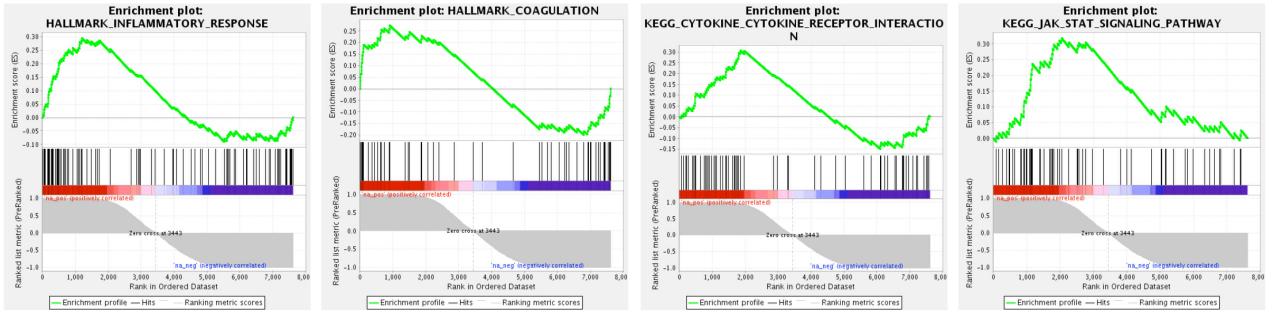

FDR q-value = 0.002
NES = 2.08

FDR q-value = 0.016
NES = 1.81

FDR q-value = 0.045
NES = 2.05

FDR q-value = 0.035
NES = 2.04

B

Pathways upregulated in mouse myCAFs vs. iCAFs & apCAFs

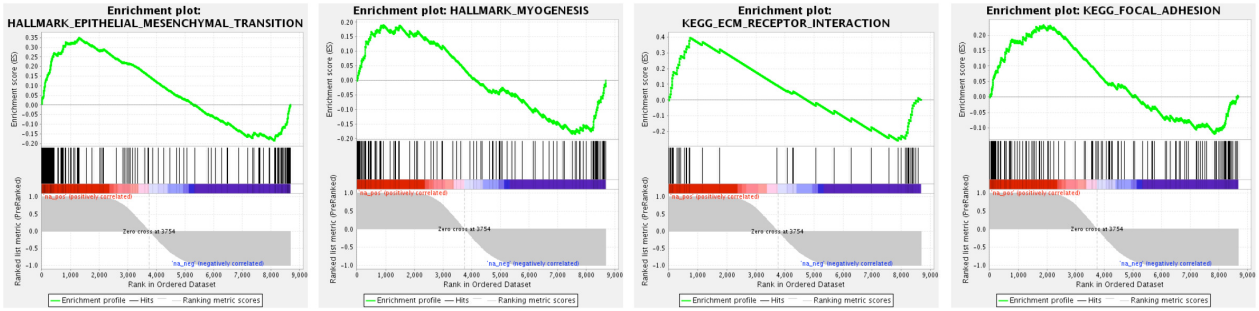

FDR q-value = 0.000
NES = 3.28

FDR q-value = 0.042
NES = 1.59

FDR q-value = 0.000
NES = 2.65

FDR q-value = 0.020
NES = 2.07

C

Pathways upregulated in mouse apCAFs vs. iCAFs & myCAFs

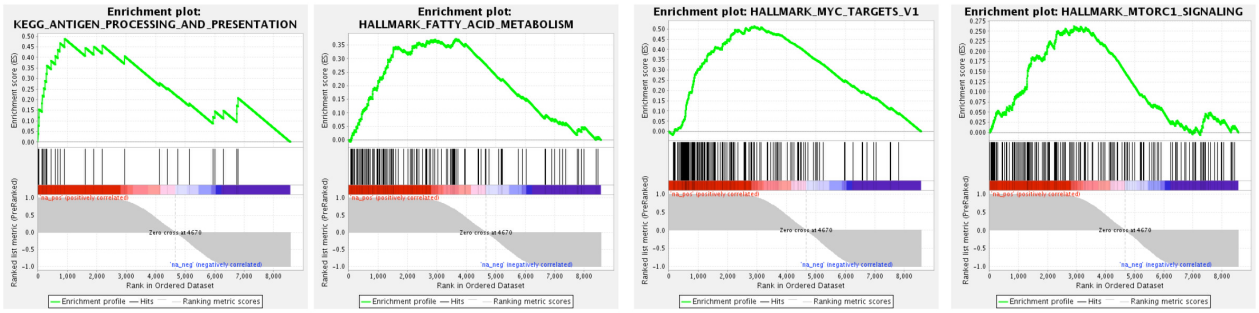

FDR q-value = 0.001
NES = 2.38

FDR q-value = 0.000
NES = 2.69

FDR q-value = 0.000
NES = 4.12

FDR q-value = 0.001
NES = 2.04

Supplementary Figure S5: Pathway analysis in different KPC CAFs. Gene set enrichment analysis (GSEA) of KPC mouse CAFs, showing upregulated pathways in iCAFs (**A**), myCAFs (**B**) and apCAFs (**C**). Each CAF subtype was compared to each of the other two subtypes, separately, and significant pathways that came up in both comparisons were selected to be shown. Histogram and significance of one of the comparisons is shown for convenience.

Figure S6

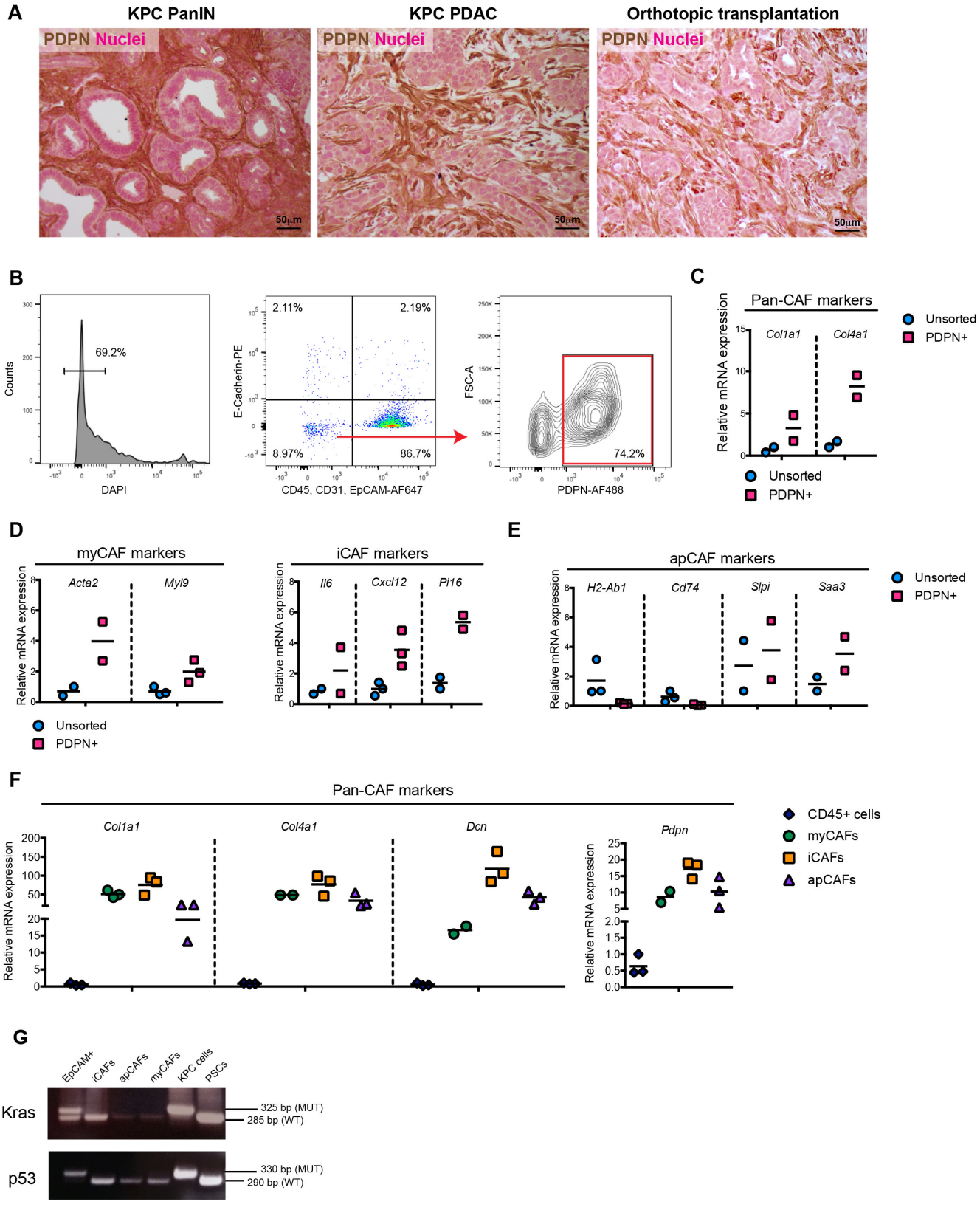
A
KPC PanIN
KPC PDAC
Orthotopic transplantation
PDPN Nuclei
50μm
B
Counts
69.2%
DAPI
2.11%
2.19%
8.97%
86.7%
E-Cadherin-PE
CD45, CD31, EpCAM-AF647
FSC-A
74.2%
PDPN-AF488
C
Pan-CAF markers
Col1a1
Col4a1
Relative mRNA expression
Unsorted
PDPN+
D
myCAF markers
Acta2
Myl9
iCAF markers
Il6
Cxcl12
Pi16
E
apCAF markers
H2-Ab1
Cd74
Slpi
Saa3
F
Pan-CAF markers
Col1a1
Col4a1
Dcn
Pdpn
CD45+ cells
myCAFs
iCAFs
apCAFs
G
EpCAM+
iCAFs
apCAFs
myCAFs
KPC cells
PSCs
Kras
325 bp (MUT)
285 bp (WT)
p53
330 bp (MUT)
290 bp (WT)

Supplementary Figure S6: Podoplanin is a pan-fibroblast marker in murine PDAC. **A.** IHC of podoplanin (PDPN) in a preneoplastic and neoplastic mouse tissue sections: KPC pancreatic intraepithelial neoplasia (PanIN, left panel), KPC PDAC (middle panel) and an orthotopic transplant model of PDAC (right panel). Nuclear Fast Red is used as counterstain. **B.** A representative FACS sorting strategy of PDPN-positive fibroblasts from a KPC tumor. Cells that were viable, negative for CD45, CD31, EpCAM and E-Cadherin, and positive for PDPN were sorted. **C-E.** qPCR analysis of pan-CAF markers (**C**) and specific CAF subtype markers (**D, E**) in PDPN^{+} sorted cells compared to unsorted population of a KPC tumor (n≥2 biological replicates). Black horizontal line represents mean value of data points. All transcripts were normalized to *Hprt*. **F.** qPCR analysis of pan-CAF markers in the three CAF subtypes sorted from KPC tumors, compared to CD45^{+} cells (n≥2 biological replicates). Black horizontal line represents mean value of data points. All transcripts were normalized to *Hprt*. **G.** PCR analysis of Kras and p53 genetic status in the different CAF subtypes, compared to EpCAM^{+} population sorted from KPC tumors. Shown is a representative example of 3 biological replicates. Bands corresponding to wild-type and recombined alleles are detected according to their different sizes. KPC cells and pancreatic stellate cells (PSCs) serve as positive controls for recombined alleles and wild-type alleles, respectively.

Figure S7

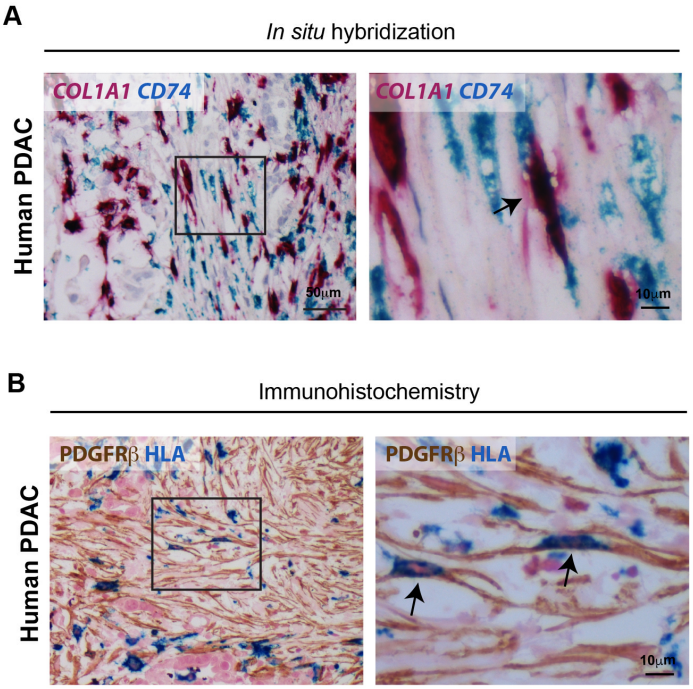

Supplementary Figure S7: Validation of apCAFs in human PDAC. A. Duplex *in situ* hybridization of *COL1A1* and *CD74* in human PDAC sections. The black square on the left panel is magnified in the right panel. Arrow indicates an apCAF. **B.** IHC of PDGFRβ and HLA-DR/DP/DQ in human PDAC sections. The black square on the left panel is magnified in the right panel. Arrows indicate apCAFs.

Figure S8

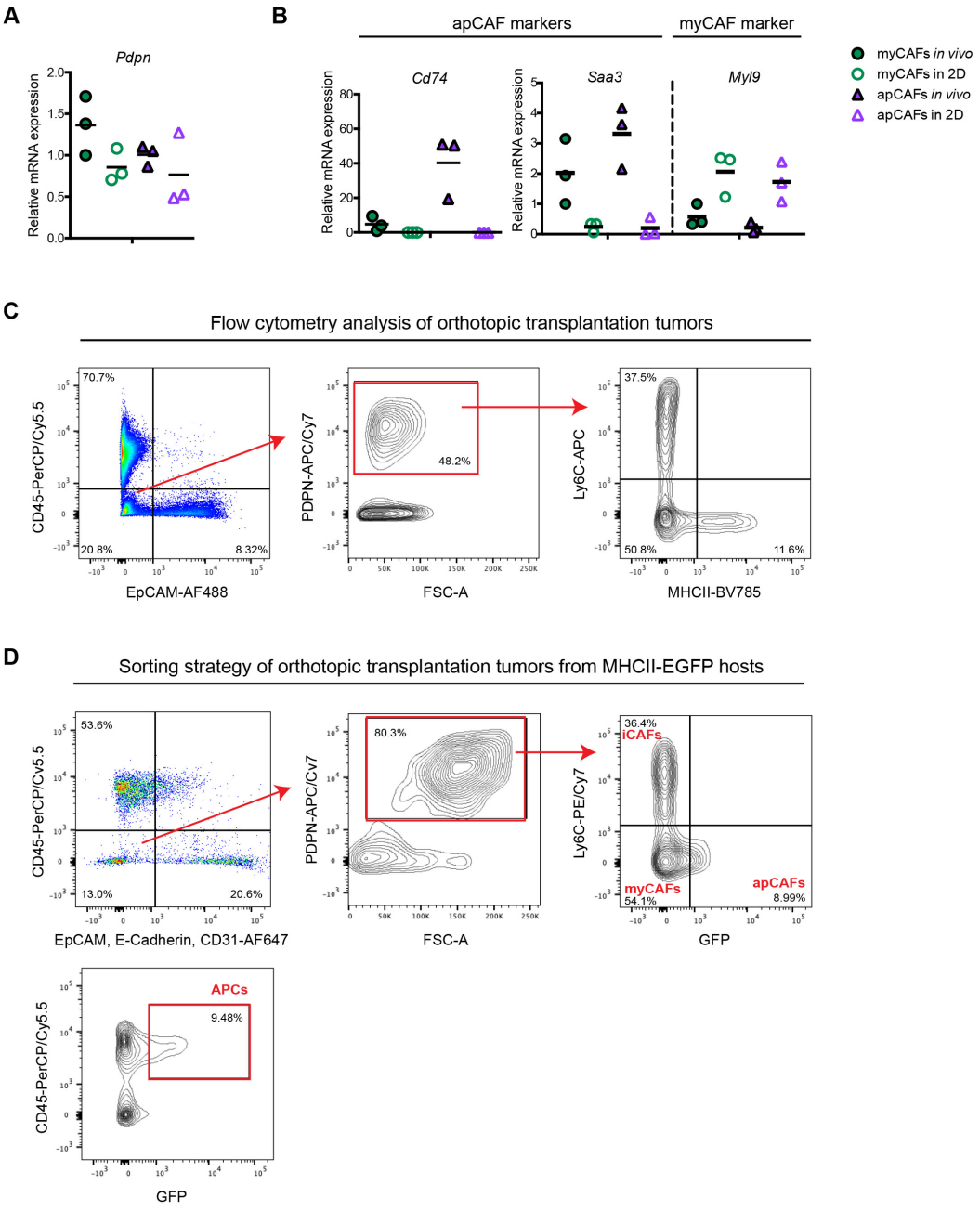

Supplementary Figure S8: Characterization of apCAFs in KPC and orthotopic transplantation models. A-B. qPCR analysis of *Pdpn* (**A**) and CAF marker genes (**B**) in apCAFs sorted from KPC tumors (apCAFs *in vivo*) compared to the same population following culture in two-dimensional monolayer (apCAFs in 2D). myCAFs sorted from the same KPC tumors (myCAFs *in vivo*) and myCAFs grown in 2D (myCAFs in 2D) were used as positive controls for myCAF genes (n=3 biological replicates). Black horizontal line represents mean value of data points. All transcripts were normalized to *Hprt*. **C.** A representative flow cytometry analysis of cell suspension from an orthotopic transplantation tumor. Forward- and side-scatter were used to eliminate debris, and DAPI staining was used to eliminate dead cells. After gating for CD45- and EpCAM-negative cells, PDPN-positive cells were stained for Ly6C and MHCII, and showed distribution into three CAF subpopulations, similar to the KPC tumors. **D.** A representative sorting strategy of orthotopic transplantation tumors from MHCII-EGFP host mice. Forward- and side-scatter were used to eliminate debris, and DAPI staining was used to eliminate dead cells. After gating for CD45-, EpCAM-, E-Cadherin- and CD31-negative cells, PDPN-positive cells were plotted for Ly6C and GFP. GFP-positive CAFs were sorted as apCAFs. In parallel, CD45-positive GFP-positive cells were sorted as professional APCs.